



Available online at <http://scik.org>

Eng. Math. Lett. 2014, 2014:14

ISSN: 2049-9337

FREE CONVECTION FLOW PAST AN IMPERMEABLE WEDGE EMBEDDED IN NANOFUID SATURATED POROUS MEDIUM WITH VARIABLE VISCOSITY BASE FLUID

MAKUNGU JAMES^{1,*}, E. W. MUREITHI², DMITRY KUZNETSOV³

¹School of Computational and Communication Science and Engineering, (NM-AIST)-Arusha, Tanzania

²Department of Mathematics, University of Dar es Salaam, Dar es Salaam, Tanzania

³Department of Mathematics, The Nelson Mandela African Institution of Science and Technology,
Arusha, Tanzania

Copyright © 2014 James, Mureithi and Kuznetsov. This is an open access article distributed under the Creative Commons Attribution License, which permits unrestricted use, distribution, and reproduction in any medium, provided the original work is properly cited.

Abstract. The paper investigates a free convection flow past an impermeable wedge embedded in nanofluid saturated porous medium. The governing partial differential equations are transformed into a set of non-linear ordinary differential equations with the help of self-similarity technique and solved using standard numerical techniques. The numerical results for the dimensionless velocity, temperature and nanoparticles volume fraction as well as the reduced Nusselt and Sherwood numbers have been analyzed and presented for various parameters, namely, viscous dissipation parameter σ , buoyancy ratio N_r , variable viscosity parameter θ_e , Brownian motion parameter N_b , thermophoresis parameter N_t , Lewis number Le and the angle of the wedge Ω . The results obtained shows that the Brownian motion, thermophoresis effects, buoyancy ratio and Lewis number significantly enhance the heat and mass transfer properties from the wall of the wedge to the fluid saturated porous medium.

Keywords: Porous medium; wedge; viscous dissipation; Convection; base fluids; variable viscosity.

2010 AMS Subject Classification: 76D05, 80A20, 76D27.

1. Introduction

*Corresponding author

Received May 17, 2014

The study of free convection of nanofluids in porous media along the heated surface has received considerable attention in recent years; that is because it is often met in many practical applications such as electronic cooling, vehicle cooling, transformer cooling, crude oil extraction, ground water pollution and so forth. An appropriate number of studies have been reported in the literature concentrating on the free convection and heat transfer in the porous media. Since the early work of Darcy in the nineteenth century, several and intensive investigations have been conducted on the laminar flow and heat transfer through porous medium, Olaseni and Olafenwa [13]. Darcy's experiment discovered that, in laminar flow through porous medium, the pressure drop caused by the frictional drag is proportional to the velocity at the low Reynolds number range. The Darcy's experiments leads to a law called Darcy law which states that, the velocity of flow of a liquid through a porous medium due to difference in pressure is proportional to the pressure gradient in the direction of flow. The law is a phenomenologically derived constitutive equation that describes the flow through a porous medium, Vafai [19] and Pop and Ingham [15]. Apart from that, nanofluids are fluids created by dispersing nanoparticles with sizes of 1-100nm in diameter in traditional heat transfer fluids such as ethylene glycol, water and oil. Yasin and Arifin [20], studied that fluids such as ethylene glycol, water and oil are poor heat transfer fluids, and therefore an alternative approaches are needed to improve the thermal conductivities of these fluids due to the fact that; the thermal conductivities play the major roles on the heat transfer coefficient between the heat transfer medium and the heat transfer surface. The nanoparticles are engineered from metals or metal oxides. Park and Choi [2], observed that copper or carbon nanotubes with 1% nanoparticle volume fractions increased the thermal conductivity of ethylene glycol or oil by 40% and 150% respectively. The increment of thermal conductivity of the base fluids in the presence of nanoparticles in the mixture is assumed to be caused by the following mechanisms; Brownian motion, thermophoresis, particle agglomeration, liquid layering on the nanoparticle-liquid interface, nanoparticle size and volume fraction. On the other hand, convectional particle-liquid suspensions require high concentrations (>10% by volume) of particles to achieve such enhancement. Since, base fluids have low thermal conductivities and metals have good thermal conductivities up to three times higher than the base

fluids, therefore there is a need to combine the two components to produce a suitable heat transfer medium that behaves like a fluid, but has the thermal properties of a metal. Many researchers have been demonstrating the nanofluids in different applications because; nanofluids are more stable, the nanoparticles spread uniformly in the base fluids and they have accepted dynamic viscosity. RamReddy et al. [16], showed that, nanofluids are smart fluids in cleaning energy and effectiveness in cooling of heated surfaces.

The problem of natural convection heat transfer of nanofluids along a vertical plate embedded in porous medium was studied by Uddin and Harmand [18]. They used an implicit finite difference scheme for a three-dimensional mesh to solve the nonlinear coupled partial differential equations. Gorla et al. [4] studied mixed convective boundary layer flow over a vertical wedge embedded in a porous medium saturated with a nanofluid by considering a natural convection dominated regime. Noghrehabadi et al. [12] studied natural convection flow of nanofluids over vertical cone embedded in non-Darcy porous media using finite difference method on collocation points and Newton's method. Rana et al. [17] studied numerical solution for mixed convection boundary layer flow of a nanofluid along an inclined plate embedded in a porous medium. Nield and Kuznetsov [11] studied the influence of nanoparticle on natural convection boundary layer flow past a vertical plate by including thermophoresis and Brownian motion in the model. A comprehensive study of natural convection was done by Moorthy et al. [10] who studied the Soret and Dufour effects on natural convection heat and mass transfer flow past a horizontal surface in a porous medium with variable viscosity. They showed that, the Nusselt number increases and Sherwood number decreases as the variable viscosity parameter approaches to zero.

Very recently, Das [3] studied the problem of natural convection of nanofluid flow past a convectively heated stretching surface using Lie group approach by taking Brownian motion and thermophoresis into consideration. Khan and Pop [8] analyzed boundary layer flow past a wedge moving in a nanofluid. They observed that the dimensionless temperature increases with both Brownian motion and thermophoresis parameters when the wedge is shrinking. Hady et al. [5] investigated the Soret effect on natural convection boundary-layer flow of a non-Newtonian nanofluid over a vertical cone embedded in a porous medium. Soret effect (thermo-diffusion)

exists when the species diffuse due to temperature different in the flow system. The effect becomes significant when the density difference exist in the flow regime. There have been several studies of the effect of temperature dependent viscosity on natural or forced boundary layer flow. Ling and Dybbs [9] investigated the forced convection with variable viscosity over flat plate in a porous medium. Hossain and Munir [6] studied combined convection from a vertical flat plate with temperature dependent viscosity and thermal conductivity. Kandasamy and Hashim [7] investigated the variable viscosity and thermophoresis effects on Darcy mixed convective heat and mass transfer past a porous wedge in the presence of chemical reaction. Piazza [14] explained that, particle thermophoresis is a nonequilibrium cross-flow effect between mass and heat transport, quite similar to thermal diffusion (the Soret effect) in simple fluid mixtures.

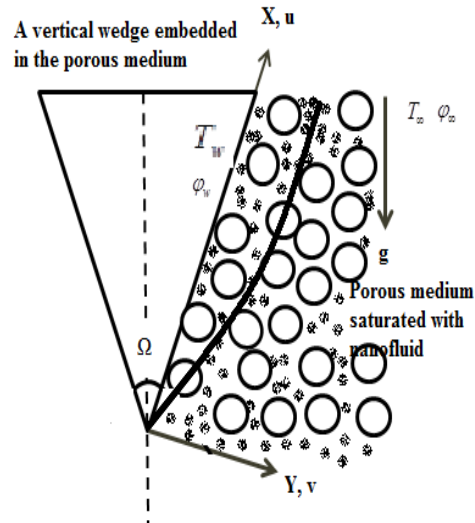


FIGURE 1. Physical model and coordinate system.

The mentioned literature survey indicates that there is no any study concerning the boundary layer flow past a vertical wedge embedded in a saturated porous medium with nanofluid, variable viscosity of the base fluid and viscous dissipation effects. Hence, in the study presented here we investigate the effects of variable viscosity of the base fluid, volume fraction of the nanoparticles, Brownian motion, thermophoresis, viscous dissipation, size of the angle of the wedge, Lewis number and buoyancy force along a wedge to the free convection problem. It is assumed that viscosity of the base fluid varies inversely as a linear function of temperature.

The problem has an important application to convective flow on the heated vertical wedge, especially in the compact design devices that cannot be cooled by the use of traditional methods rather than using nanoparticle material for enhancing thermal conductivity of the base fluids. Furthermore, the paper is organised in the following manner. Section two presents the problem formulation, Section three is presented the numerical technique. Section four will discuss the results and discussion and finally conclusion is made in Section five.

2. Problem Formulation

The current problem considers the steady convection boundary layer flow of a nanofluid over an impermeable wedge embedded in a porous medium with temperature dependent viscosity and viscous dissipation. The impermeable wedge is placed vertically in the porous medium filled with the nanofluid as shown in Fig 1. The coordinate is selected in such a way that the x-axis is aligned with the flow on the surface of the vertical wedge and the y-axis is taken normal to it. The system is governed by continuity, momentum, energy and concentration equations in two dimensional laminar flow of nanofluid. The Darcy model is used to describe the flow of nanofluid in porous medium with small porosity and low flow within the porous medium. As shown in Fig 1, the slant surface temperature T and the nanoparticle fraction volume take values T_w and ϕ_w , respectively. The ambient values, attained as y tends to infinity are T_∞ and ϕ_∞ , respectively. It is assumed that the convective nanofluid and the porous medium are in local thermodynamic equilibrium. Also, it is assumed that the physical properties of the base fluid and that of the nanoparticles are constant except the density of the fluid at the buoyancy term, so that the Oberbeck-Boussinesq approximation holds. Furthermore, the base fluid viscosity varies inversely with temperature and the flow of the nanofluid past a wedge is assumed to satisfy the slip condition. Following the nanofluid equations proposed by Noghrehabadi et al. [12] together with the boundary layer approximation, the basic equations for laminar, steady-state, viscous and incompressible flow can be written as follows;

$$(1) \quad \frac{\partial u}{\partial x} + \frac{\partial v}{\partial y} = 0.$$

$$(2) \quad \frac{\mu(T)}{K}u = -\frac{\partial p}{\partial x} + (1 - \varphi_\infty)\beta g\rho_{f\infty}(T - T_\infty)\cos\left(\frac{\Omega}{2}\right) - (\rho_p - \rho_{f\infty})g(\varphi - \varphi_\infty)\cos\left(\frac{\Omega}{2}\right).$$

$$(3) \quad \frac{\partial p}{\partial y} = 0.$$

$$(4) \quad (\rho c_p)_f \left(u \frac{\partial T}{\partial x} + v \frac{\partial T}{\partial y} \right) = k_m \frac{\partial^2 T}{\partial y^2} + \varepsilon (\rho c_p)_p \left(D_B \frac{\partial \varphi}{\partial y} \frac{\partial T}{\partial y} + \frac{D_T}{T_\infty} \left(\frac{\partial T}{\partial y} \right)^2 \right) + \frac{\mu(T)}{K}u^2.$$

$$(5) \quad \frac{1}{\varepsilon} \left(u \frac{\partial \varphi}{\partial x} + v \frac{\partial \varphi}{\partial y} \right) = D_B \frac{\partial^2 \varphi}{\partial y^2} + \frac{D_T}{T_\infty} \frac{\partial^2 T}{\partial y^2}.$$

In Eqns (1-5), u and v are Darcy velocity components along x and y axes, respectively; ρ , $\mu(T)$ and β are the density, variable dynamic viscosity and thermal expansion coefficient of the base fluid; $(\rho c_p)_p$ and $(\rho c_p)_f$ are the effective heat capacity of the nanofluid and heat capacity of the base fluid; ε and K are the porosity and permeability of the porous medium; χ and α_m are the heat capacity ratio and thermal diffusivity in the porous material; T and φ are the local temperature and nanoparticle volume fraction within the boundary layer. Furthermore, k_m is an effective thermal conductivity of the porous medium, while D_T , D_B and g are the thermophoretic diffusion coefficient, Brownian diffusion coefficient and gravitational acceleration respectively. The Eqns (1-5) are subjected to the following boundary conditions;

$$(6) \quad y = 0, x \geq 0, v = 0, T = T_w, \varphi = \varphi_w.$$

$$(7) \quad y \rightarrow \infty, x \geq 0, u = 0, T = T_\infty, \varphi = \varphi_\infty.$$

Equations (2) and (3) are simplified by employing cross-differentiation technique together with a stream line function (Ψ), that satisfies the continuity equation:

$$(8) \quad u = \frac{\partial \Psi}{\partial y}, \quad v = -\frac{\partial \Psi}{\partial x}.$$

The governing non-linear partial differential Equations (2 – 5) are then reduced to the following equations;

$$(9) \quad \frac{\partial}{\partial y} \left(\frac{\mu(T)}{K} \frac{\partial \Psi}{\partial y} \right) = (1 - \varphi_\infty)\beta g\rho_{f\infty} \frac{\partial T}{\partial y} \cos\left(\frac{\Omega}{2}\right) - (\rho_p - \rho_{f\infty})g \frac{\partial \varphi}{\partial y} \cos\left(\frac{\Omega}{2}\right).$$

$$(10) \quad \frac{\partial \Psi}{\partial y} \frac{\partial T}{\partial x} - \frac{\partial \Psi}{\partial x} \frac{\partial T}{\partial y} = \alpha_m \frac{\partial^2 T}{\partial y^2} + \chi \left(D_B \frac{\partial \phi}{\partial y} \frac{\partial T}{\partial y} + \frac{DT}{T_\infty} \left(\frac{\partial T}{\partial y} \right)^2 \right) + \frac{1}{(\rho c_p)_f} \frac{\mu(T)}{K} \left(\frac{\partial \Psi}{\partial y} \right)^2.$$

$$(11) \quad \frac{\partial \Psi}{\partial y} \frac{\partial \phi}{\partial x} - \frac{\partial \Psi}{\partial x} \frac{\partial \phi}{\partial y} = \varepsilon D_B \frac{\partial^2 \phi}{\partial y^2} + \frac{\varepsilon D_T}{T_\infty} \frac{\partial^2 T}{\partial y^2},$$

where

$$(12) \quad \alpha_m = \frac{k_m}{(\rho c_p)_f}, \quad \chi = \frac{(\rho c_p)_p}{(\rho c_p)_f}.$$

For the present base fluid, following [1], the dynamic viscosity of the base fluid is considered in the following form:

$$(13) \quad \mu_f(T) = \frac{\mu_\infty}{1 + \gamma(T - T_\infty)} = \frac{1}{a(T - T_e)},$$

where μ_∞ is a dynamic viscosity of the ambient base fluid; γ is a constant value, it implies that when $\gamma = 0$, the dynamic viscosity of the base fluid flow remains constant throughout the system. Apart from that, a and T_e are constants, given by

$$(14) \quad a = \frac{\gamma}{\mu_\infty}, \quad T_e - T_\infty = -\frac{1}{\gamma}.$$

We now look for similarity solutions of Equations (9-11) with the boundary conditions (6) and (7) of the following form;

$$(15) \quad \eta = \frac{y}{x} Ra_x^{1/2}, \quad \Psi(x, y) = \alpha_m Ra_x^{1/2} f(\eta), \quad \theta = \frac{T - T_\infty}{T_w - T_\infty}, \quad C = \frac{\phi - \phi_\infty}{\phi_w - \phi_\infty}, \quad \theta_e = \frac{T_e - T_\infty}{T_w - T_\infty}$$

given that, $Ra_x = \frac{(1 - \phi_\infty) \rho_{f\infty} \beta g K x (T_w - T_\infty)}{\mu_\infty \alpha_m}$ is the local Rayleigh number of the porous medium, θ_e

and T_e are variable viscosity parameter and reference temperature in the boundary layer flow.

Substituting the Eqns (13) and (15) in Eqns (9-11), we get the following system of non-linear ordinary differential equations:

$$(16) \quad f'' + \frac{f' \theta'}{(\theta_e - \theta)} - \left(\frac{\theta_e - \theta}{\theta_e} \right) (\theta' - N_r C') \cos \left(\frac{\Omega}{2} \right) = 0.$$

$$(17) \quad \theta'' + \frac{1}{2} f \theta' + N_b C' \theta' + N_t (\theta')^2 + \sigma \frac{\theta_e}{(\theta_e - \theta)} (f')^2 = 0.$$

$$(18) \quad C'' + \frac{1}{2}Le f C' + \frac{N_t}{N_b} \theta'' = 0.$$

Subjected to the following boundary conditions:

$$(19) \quad \begin{aligned} \eta = 0, f(0) = 0, \theta(0) = 1, C(0) = 1 \\ \eta \rightarrow \infty, f' = 0, \theta = 0, C = 0, \end{aligned}$$

where primes represent the derivative with respect to η . In Eqns (16-18) the emerged parameters are defined as follows;

$$(20) \quad \begin{aligned} N_r = \frac{(\rho_p - \rho_{f\infty})(\varphi_w - \varphi_\infty)}{(1 - \varphi_\infty)(T_w - T_\infty)\rho_{f\infty}\beta}, \quad N_b = \frac{\varepsilon(\rho c_p)_p D_B(\varphi_w - \varphi_\infty)}{(\rho c_p)_f \alpha_m}, \\ N_t = \frac{\varepsilon(\rho c_p)_p D_T(T_w - T_\infty)}{(\rho c_p)_f T_\infty \alpha_m}, \quad \sigma = \frac{\mu_\infty \alpha_m Ra_x}{K(\rho c_p \rho)_f(T_w - T_\infty)}, \quad Le = \frac{\alpha_m}{\varepsilon D_B}, \end{aligned}$$

where N_r is a buoyancy ratio number; N_b is a Brownian motion parameter; N_t is a thermophoresis parameter; σ is a viscous dissipation parameter and Le is a Lewis number. It has showed that θ_e is determined by the viscosity/temperature characteristics of the base fluid and the operating temperature difference is $\Delta T = T_w - T_\infty$ or $\theta_e = -1/\gamma(T_w - T_\infty)$. It is also shown that, if $|\theta_e|$ is small then either the base fluid viscosity changes with temperature difference or the temperature difference is high. It may be noted that for assisting flow θ_e is negative for liquids and positive for gases Abdelgaied and Eid [1].

The quantities of physical interest are local Nusselt number Nu_x and local Sherwood number Sh_x , which are defined as follows:

$$(21) \quad Nu_x = \frac{h_w x}{k_m} = \frac{q_w'' x}{k_m(T_w - T_\infty)} = -\frac{x \frac{\partial T}{\partial y}}{(T_w - T_\infty)},$$

$$(22) \quad Sh_x = \frac{h_m x}{D} = \frac{q_m'' x}{D(\varphi_w - \varphi_\infty)} = -\frac{x \frac{\partial \varphi}{\partial y}}{(\varphi_w - \varphi_\infty)},$$

where q_w'' , q_m'' , h_w and h_m are heat transfer rate, mass transfer rate, heat transfer coefficient and mass transfer coefficient at the slant surface of a wedge respectively. Furthermore, using similarity variables mentioned in Eqn (15), the new expressions of reduced Nusselt number and reduced Sherwood number are obtained as follows;

$$(23) \quad Nu_x = -Ra_x^{\frac{1}{2}} \left(\theta'(0) \right), \quad Sh_x = -Ra_x^{\frac{1}{2}} \left(C'(0) \right).$$

$$(24) \quad Nu_r = \frac{Nu_x}{Ra_x^{\frac{1}{2}}} = -\theta'(0), \quad Sh_r = \frac{Sh_x}{Ra_x^{\frac{1}{2}}} = -C'(0).$$

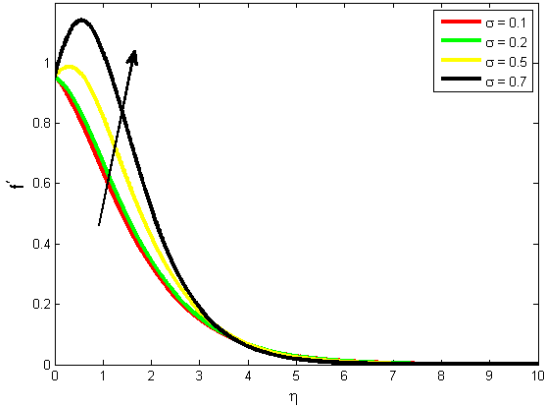
3. Numerical technique

The non-linear ordinary differential equations (16), (17) and (18) together with the boundary conditions (19) have been solved numerically by employing the fourth order Runge-Kutta technique alongside with shooting method. The proper guessing of $f'(0)$, $\theta'(0)$ and $C'(0)$ was done with the help of shooting technique. Apart from that, the step size of $\Delta\eta = 0.001$ and the accuracy of 10^{-8} as the criterion of convergence were used to get the numerical solutions. The computations have been done using various parameter values. The following parameters were considered, namely, viscous dissipation parameter σ , variable viscosity θ_e , buoyancy parameter N_r , thermophoresis parameter N_t , Brownian motion parameter N_b , size of a wedge Ω and Lewis number Le . The dimensionless velocity, temperature, nanoparticle volume fraction, reduced Nusselt and reduced Sherwood profiles were presented in graphical forms. In the following section, the effects of the parameters governing the problem are explained in detail.

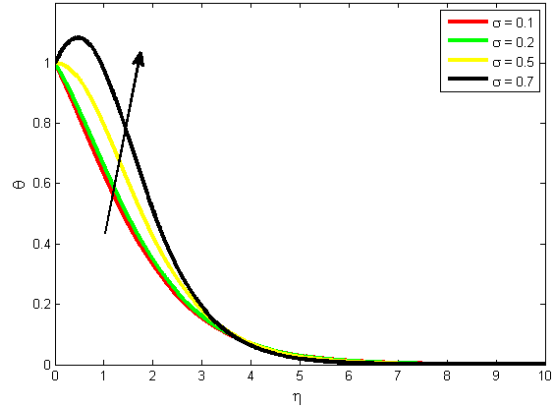
4. Results and Discussion

In our current study, we have solved numerically and analyzed the theoretical solutions of the dimensionless Equations (16-18) subjected to the boundary conditions (19) and Equation (24) for reduced Nusselt number and reduced Sherwood number respectively. Numerical analysis are carried out for $-1000 \leq \theta_e \leq -10$, $0.1 \leq \sigma < 0.8$, $0.1 \leq N_r \leq 0.5$, $0 \leq N_b \leq 0.5$, $0.1 \leq N_t \leq 0.5$, $10 \leq Le \leq 100$ and $0 \leq \Omega \leq \frac{\pi}{6}$. The effects of various parameters on the dimensionless velocity, temperature, nanoparticle volume fraction, reduced Nusselt number and reduced Sherwood number in the boundary layer flow have shown in graphical form. A detail elaboration is provided for every parameter involved in the simulation.

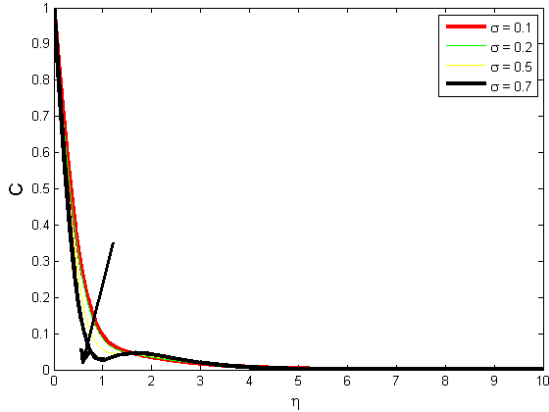
The effect of viscous dissipation parameter σ on velocity, temperature and nanoparticle volume fraction profiles are shown in Figs (a), (b) and (c) respectively for fixed θ_e , N_r , N_b , N_t ,



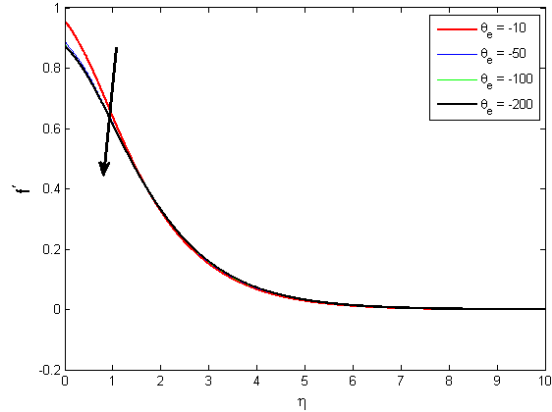
(a) Effects of viscous dissipation parameter σ on velocity profiles with $\theta_e = -10$, $N_r = 0.1$, $N_b = 0.1$, $N_t = 0.1$, $Le = 10$, $\Omega = \pi/6$.



(b) Effects of viscous dissipation parameter σ on temperature profiles with $\theta_e = -10$, $N_r = 0.1$, $N_b = 0.1$, $N_t = 0.1$, $Le = 10$, $\Omega = \pi/6$.



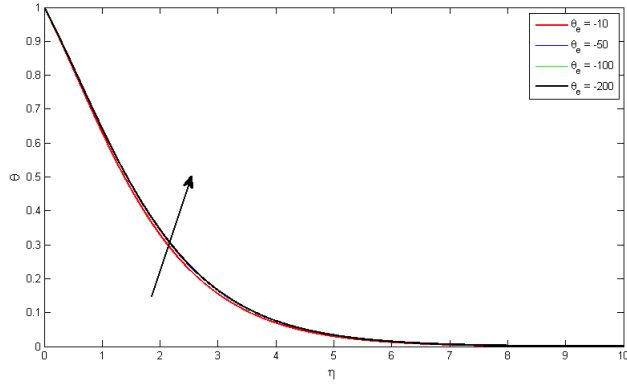
(c) Effects of viscous dissipation parameter σ on nanoparticle volume fraction profiles with $\theta_e = -10$, $N_r = 0.1$, $N_b = 0.1$, $N_t = 0.1$, $Le = 10$, $\Omega = \pi/6$.



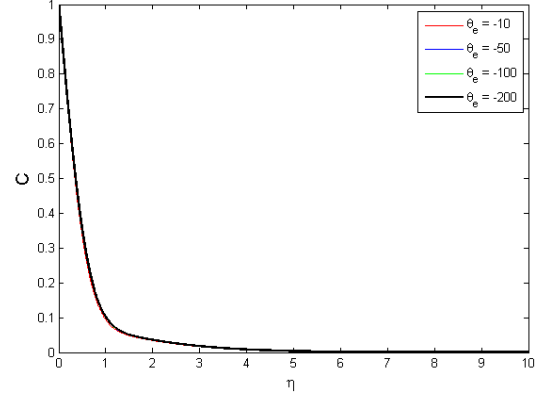
(d) Effects of variable viscosity parameter θ_e on velocity profiles with $\sigma = 0.1$, $N_r = 0.1$, $N_b = 0.1$, $N_t = 0.1$, $Le = 10$, $\Omega = \pi/6$.

Le and Ω . In Fig (a), it is observed that as the viscous dissipation parameter increases, dimensionless velocity in the boundary layer flow increases. Here, we concluded that, the increase in velocity of the nanofluid is caused by the decrease of density of the nanofluid in the boundary layer due to the heat generated by viscous flow. From Fig (b) it is evident that the temperature increase as viscous dissipation parameter increases, while in Fig (c), it is observed that as the viscous dissipation parameter increases, dimensionless nanoparticle volume fraction decreases. This is due to the fact that, the heat generated in the boundary layer by viscous dissipation acts

as a barrier for the nanoparticles to move from a wedge to the fluid (thermophoresis effect is insignificant in this case). In Figs (d), (e) and (f) the dimensionless velocity, temperature and

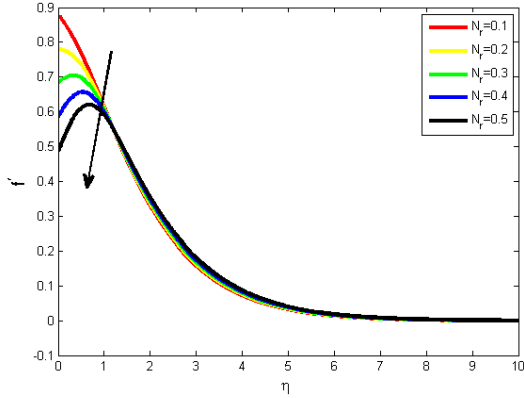


(e) Effects of variable viscosity parameter θ_e on temperature profiles with $\sigma = 0.1, N_r = 0.1, N_b = 0.1, N_t = 0.1, Le = 10, \Omega = \pi/6$.

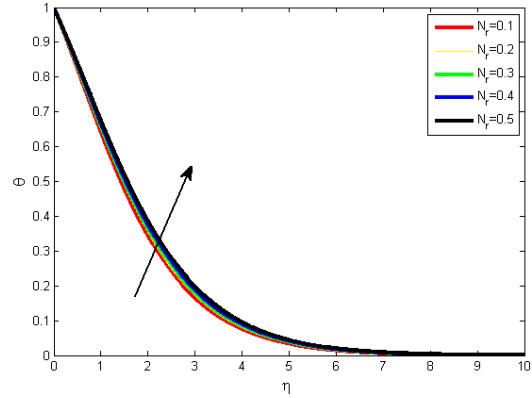


(f) Effects of variable viscosity parameter θ_e on nanoparticle volume fraction profiles with $\sigma = 0.1, N_r = 0.1, N_b = 0.1, N_t = 0.1, Le = 10, \Omega = \pi/6$.

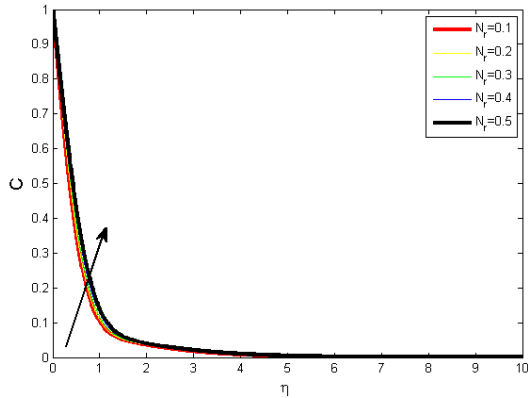
nanoparticle volume fraction are plotted against the similarity variable η for different values of variable viscosity parameter. It is observed that, as the variable viscosity parameter increases $|\theta_e|$, the dimensionless velocity decreases as shown in Fig (d). The decreasing velocity of the nanofluid near the wedge is due to the small difference in temperatures at the wedge and that at the ambient as $\theta_e \rightarrow -\infty$. From Fig (e), it is observed that as variable viscosity parameter increases $|\theta_e|$, the dimensionless temperature increases. However, no significant effects have been observed in the nanoparticle volume fraction for absolute increasing the variable viscosity parameters as shown in Fig (f) for fixed $\sigma, N_r, N_b, N_t, Le$ and Ω . The buoyancy ratio N_r is a basic parameter for the free convection heat and mass transfer in the boundary layer flow. Figures (g), (h) and (i) illustrate the dimensionless velocity, temperature and nanoparticle volume fraction profiles for different values of N_r . In Fig (g), it is observed that as the buoyancy ratio parameter increases, the velocity of the nanofluid in the boundary layer decreases. This is due to the fact that, the induced buoyancy force of the nanoparticle opposes the thermal buoyancy force as a result the velocity of the flow decrease. However, both temperature and nanoparticle volume fraction profiles increase as the buoyancy ratio parameter increases as shown in Figs (h) and (i) for fixed $\sigma, \theta_e, N_b, N_t, Le$ and Ω . Figures (j), (k) and (l) illustrate the dimensionless



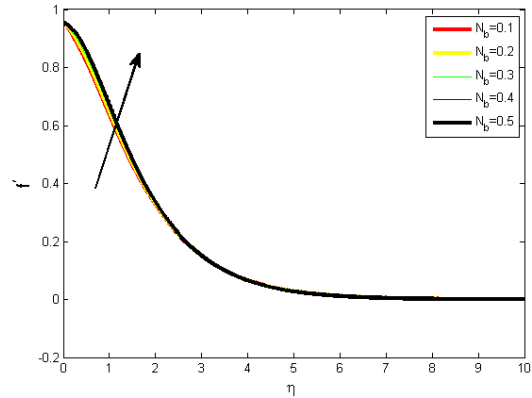
(g) Effects of buoyancy ratio number N_r on velocity profiles with $\sigma = 0.1$, $\theta_e = -100$, $N_b = 0.1$, $N_t = 0.1$, $Le = 10$, $\Omega = \pi/6$.



(h) Effects of buoyancy ratio number N_r on temperature profiles with $\sigma = 0.1$, $\theta_e = -100$, $N_b = 0.1$, $N_t = 0.1$, $Le = 10$, $\Omega = \pi/6$.

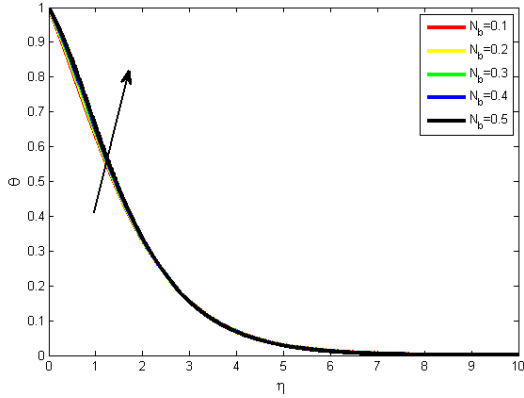


(i) Effects of buoyancy ratio number N_r on nanoparticle volume fraction profiles with $\sigma = 0.1$, $\theta_e = -100$, $N_b = 0.1$, $N_t = 0.1$, $Le = 10$, $\Omega = \pi/6$.

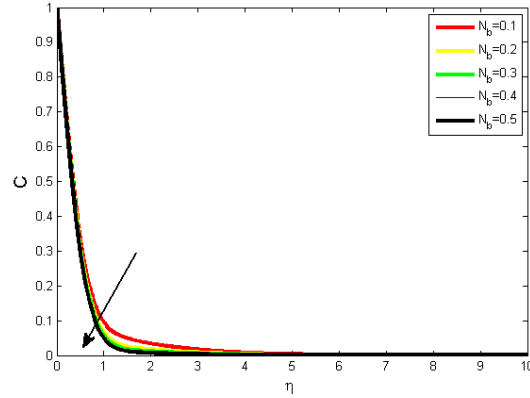


(j) Effects of Brownian motion parameter N_b on velocity profiles with $\sigma = 0.1$, $\theta_e = -10$, $N_r = 0.1$, $N_t = 0.1$, $Le = 10$, $\Omega = \pi/6$.

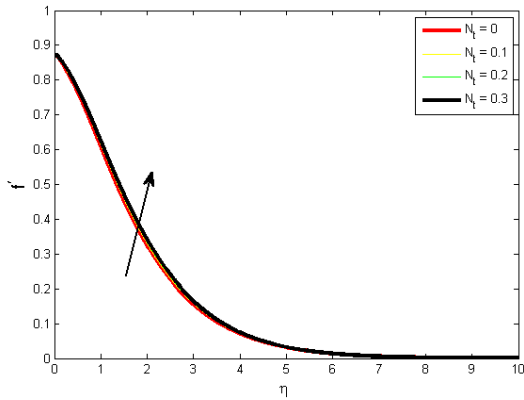
velocity, temperature and nanoparticle volume fraction by various Brownian motion parameters N_b for fixed σ , N_r , N_t , θ_e , Le and Ω . From the Figures (j) and (k), it is realised that as the Brownian motion parameter increases, both the velocity and temperature distributions in the boundary layer increases and decreases for the nanoparticle volume fraction as shown in the Fig (l). In nanofluid flow, the Brownian motion of the nanoparticles plays a major role in heat transfer from a heated surface to the fluids. Figures (m), (n) and (o) display the effect of thermophoresis parameter N_t on the dimensionless velocity, temperature and nanoparticle volume



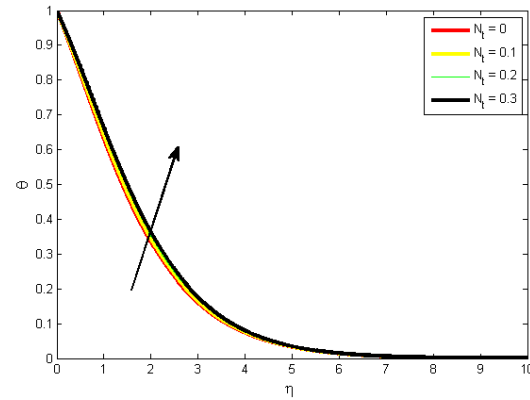
(k) Effects of Brownian motion parameter N_b on temperature profiles with $\sigma = 0.1$, $\theta_e = -10$, $N_r = 0.1$, $N_t = 0.1$, $Le = 10$, $\Omega = \pi/6$.



(l) Effects of Brownian motion parameter N_b on nanoparticle profiles with $\sigma = 0.1$, $\theta_e = -10$, $N_r = 0.1$, $N_t = 0.1$, $Le = 10$, $\Omega = \pi/6$.

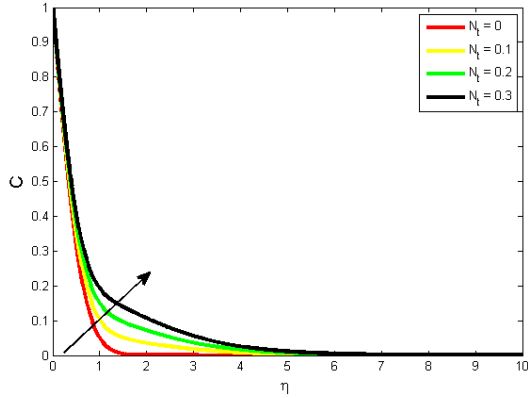


(m) Effects of thermophoresis parameter N_t on velocity profiles with $\sigma = 0.1$, $\theta_e = -10$, $N_r = 0.1$, $N_b = 0.1$, $Le = 10$, $\Omega = \pi/6$.

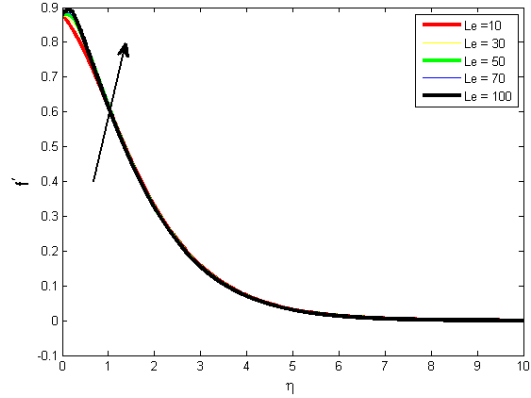


(n) Effects of thermophoresis parameter N_t on temperature profiles with $\sigma = 0.1$, $\theta_e = -10$, $N_r = 0.1$, $N_b = 0.1$, $Le = 10$, $\Omega = \pi/6$.

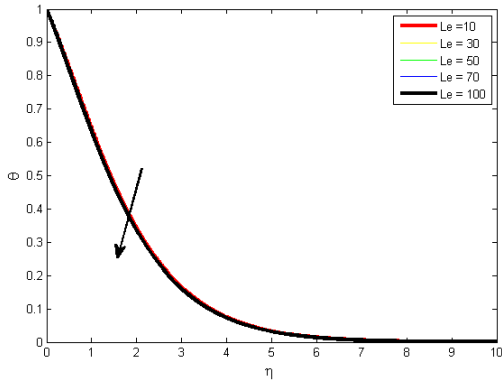
fraction for fixed σ , N_r , N_b , Le , θ_e and Ω . In both Figs, it is shown that as thermophoresis parameter increases both dimensionless velocity, temperature and nanoparticle volume fraction profiles increase in the boundary layer. This is due to the fact that, for heated surface thermophoresis phenomenon tends to blow or upset the nanoparticles from the heated surface to the fluid, since a heated surface repels the nanometer size particles from it to the flowing fluid. Therefore, the thermophoretic force enables nanoparticles to carry heat from the surface to the moving fluids. This leads to increase the velocity, temperature and nanoparticle volume fraction in the boundary layer flow. The effects of various Lewis number Le on velocity, temperature



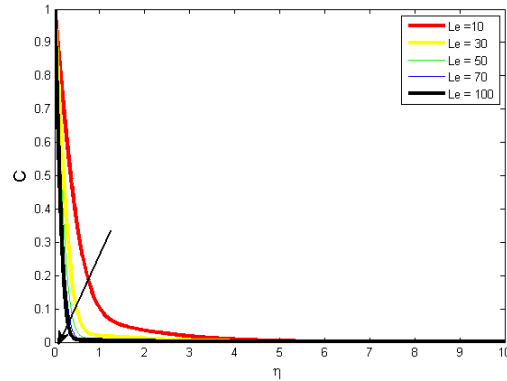
(o) Effects of thermophoresis parameter N_t on nanoparticle volume fraction profiles with $\sigma = 0.1$, $\theta_e = -10$, $N_r = 0.1$, $N_b = 0.1$, $Le = 10$, $\Omega = \pi/6$.



(p) Effects of Lewis number Le on velocity profiles with $\sigma = 0.1$, $\theta_e = -100$, $N_r = 0.1$, $N_b = 0.1$, $N_t = 0.1$, $\Omega = \pi/6$.

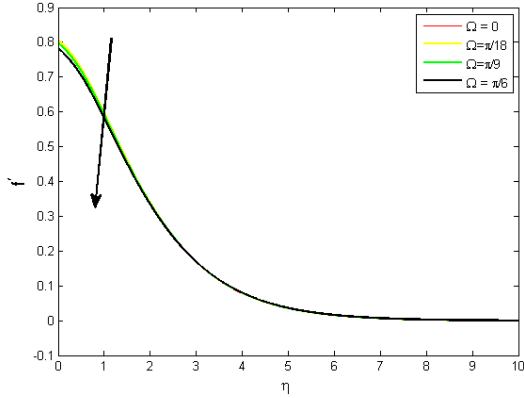


(q) Effects of Lewis number Le on temperature profiles with $\sigma = 0.1$, $\theta_e = -100$, $N_r = 0.1$, $N_b = 0.1$, $N_t = 0.1$, $\Omega = \pi/6$.

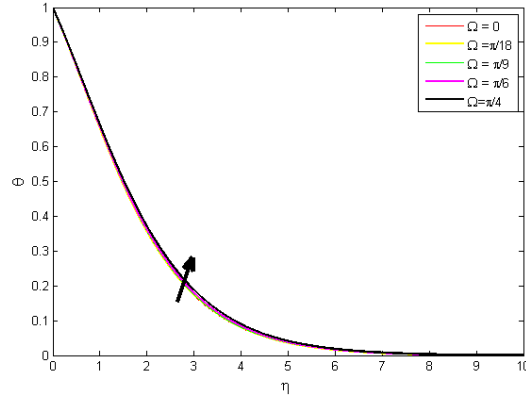


(r) Effects of Lewis number Le on nanoparticle volume fraction profiles with $\sigma = 0.1$, $\theta_e = -100$, $N_r = 0.1$, $N_b = 0.1$, $N_t = 0.1$, $\Omega = \pi/6$.

and nanoparticle volume fraction have shown in Figures (p), (q) and (r) for fixed σ , N_r , N_b , N_t , θ_e and Ω . In Fig (p), it is observed that as Le increases the velocity of the nanofluid is slightly increases in the boundary layer flow. However, both temperature and nanoparticle volume fraction decreases as the lewis number increases as shown in Figures (q) and (r). Figures (s) and (t) illustrate the dimensionless velocity and temperature by various angles of the wedge for fixed σ , N_r , N_b , N_t , Le and Ω . From Fig (s), it is observed that as the angle of the wedge increases, the velocity of the flow decreases. This is caused by the component of gravitational acceleration

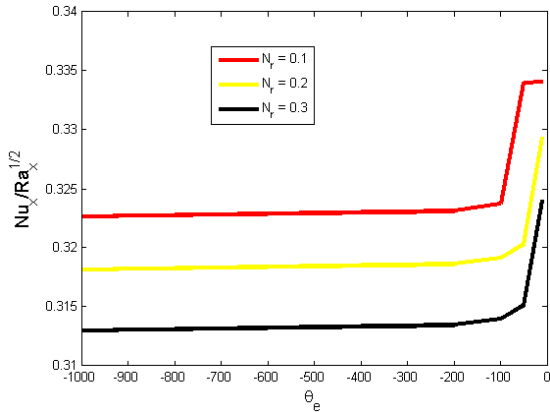


(s) Effects of angle of a wedge Ω on velocity profiles with $\sigma = 0.1$, $\theta_e = -10$, $N_r = 0.1$, $N_b = 0.1$, $N_t = 0.1$, $Le = 10$.

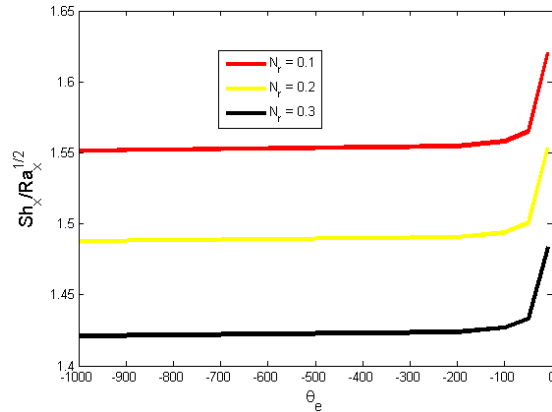


(t) Effects of angle of a wedge Ω on temperature profiles with $\sigma = 0.1$, $\theta_e = -10$, $N_r = 0.1$, $N_b = 0.1$, $N_t = 0.1$, $Le = 10$

acting on the fluid flow to be less than the actual value. However, in Fig (t), it is realised that as the fluid decelerate in the boundary, the temperature increases near the wedge.



(u) Effects of buoyancy ratio parameter N_r on the rate of heat transfer for different values of θ_e , with $N_b = 0.1$, $N_t = 0.1$, $Le = 10$, $\Omega = \pi/6$, $\sigma = 0.1$.



(v) Effects of buoyancy ratio parameter N_r on the rate of mass transfer for different values of θ_e , with $N_b = 0.1$, $N_t = 0.1$, $Le = 10$, $\Omega = \pi/6$, $\sigma = 0.1$.

In Figures (u) and (v) we noted that as buoyancy ratio parameter N_r increases, the rate of heat transfer (reduced Nusselt number) and the rate of nanoparticle volume fraction transfer (reduced Sherwood number) decrease. The numerical values are shown in Tables (1) and (2).

5. Conclusions

TABLE 1. Numerical values of dimensionless reduced Nusselt numbers for various values of θ_e and N_r with $N_b = 0.1$, $\sigma = 0.1$, $N_t = 0.1$, $Le = 10$, $\Omega = \pi/6$

θ_e	$N_r = 0.1$	$N_r = 0.2$	$N_r = 0.3$
-10	0.33410	0.32939	0.32402
-50	0.33402	0.32035	0.31516
-100	0.32375	0.31920	0.31403
-200	0.32316	0.31863	0.31346
-1000	0.32270	0.31817	0.31301

TABLE 2. Numerical values of dimensionless reduced Sherwood numbers for various values of θ_e and N_r with $N_b = 0.1$, $\sigma = 0.1$, $N_t = 0.1$, $Le = 10$, $\Omega = \pi/6$

θ_e	$N_r = 0.1$	$N_r = 0.2$	$N_r = 0.3$
-10	1.62054	1.55363	1.48377
-50	1.56537	1.50088	1.43354
-100	1.55834	1.49416	1.42715
-200	1.55481	1.49078	1.42394
-1000	1.55198	1.48808	1.42136

In this paper, we analyzed a free convection flow past an impermeable wedge embedded in nanofluid saturated porous medium with variable viscosity base fluid. The effects of various parameters, namely, variable viscosity θ_e , buoyancy ratio N_r , thermophoresis parameter N_t , viscous dissipation parameter σ , Brownian motion N_b and Lewis number Le on the flow have been analyzed and presented in graphical forms. Numerical results for surface heat transfer rate ($Nu_x/Ra_x^{1/2} = -\theta'(0)$) and nanoparticle volume fraction transfer rate ($Sh_x/Ra_x^{1/2} = -C'(0)$) have been presented for various variable viscosity parameters θ_e and buoyancy ratio parameter N_r . It is realised that the viscous dissipation parameter σ , has strong impact to the rate of heat transfer from the heated wedge. We resolved that the viscous dissipation parameter σ must be minimized in the system in order to enhance the heat and mass transfer from the wedge to the fluid flow. Furthermore, the variable viscosity parameter θ_e should be reduced to enhance heat and mass transfer from the wedge. Also, we noted that the thermophoresis process and

Brownian motion are very important in the heat and mass transfer from the wedge to the fluid flow, if and only if the viscous dissipation effect reduced in the flow by increasing the porosity ε of the porous medium.

Conflict of Interests

The authors declare that there is no conflict of interests.

REFERENCES

- [1] S. M. Abdelgaied, M. R. Eid, Mixed convection flow of nanofluids over a vertical surface embedded in a porous medium with temperature dependent viscosity. *Recent advances in mathematical methods and computational techniques in modern science*, 3 (2013), 300-312.
- [2] S. P. Anjali, A. Julie, Laminar boundary layer flow of nanofluid over a flat plate, *Int. J. Appl. Math. Mech.* 7 (2011),52-71.
- [3] K. Das, Lie group analysis for nanofluid flow past a convectively heated stretching surface, *Appl. Math. Comput.* 221 (2013), 547-557.
- [4] R.S.M. Gorla, A.J. Chamkha, A. M. Rashad, Mixed convective boundary layer flow over a vertical wedge embedded in a porous medium saturated with a nanofluid. natural convection dominated regime. *Nanoscale Research Lett.* 2011 (2011), 2-207.
- [5] F. M. Hady, R. M. Eid, M. R. Abd-Elsalam, A. M. Ahmed, Soret effect on natural convection boundary-layer flow of a non-newtonian nanofluid over a vertical cone embedded in a porous medium, *IOSR J. Math.* 8 (2013), 51-61.
- [6] M. Hossain, M. Munir, Combined convection from a vertical flate with temperature dependent viscosity and thermal conductivity, *International Journal of Fluid Mechanics Research*, (2002).
- [7] M. R. Kandasamy, I. Hashim, Variable viscosity and thermophoresis effectson darcy mixed convective heat and mass transfer past a porous wedge in the presence of chemical reaction. *Theoret. Appl. Mech.* 36 (2009), 29-46.
- [8] W. A. Khan, I.Pop, Boundary layer flow past a wedge moving in a nanofluid. *Mathematical problem in Engineering*, 2013 (2013), Article ID 637285.
- [9] J. X. Ling, A. Dybbs, Forced convection over a flat plate submerged in a porous medium: variable viscosity case. *Recent Avances in Mathematical Methods and Computational Techniques in Modern science*, ASME paper87-WA/HT-23(1987), 13-18.

- [10] M. B. K. Moorthy, T. Kannan, K. Senthilvadivu, Soret and Dufour effects on natural convection heat and mass transfer flow past a horizontal surface in a porous medium with variable viscosity, *Wseas Transactions on Heat and Mass Transfer*, (2013).
- [11] D. A. Nield, A. V. Kuznetsov, Natural convection boundary layer of a nanofluid past a vertical plate, *Int. J. Therm. Sci.* 49 (2010), 243-247.
- [12] A. Noghrehabadi, A. Behseresht, M. Ghalambaz, Natural convection flow of nanofluids over vertical cone embedded in non-darcy porous media, *Journal of Thermophysics and Heat Transfer* (2013).
- [13] T. L. Olaseni, R. Olafenwa, Analytical solution of a steady non-reacting laminar fluid flow in a chemical filled with saturated porous media with two distinct horizontal impermeable wall conditions, *Journal of Natural Sciences Research*, (2006).
- [14] R. Piazza, Thermophoresis: Moving particles with thermal gradients, *The Royal Society of Chemistry*, 4 (2008), 1740-1744.
- [15] I. Pop, D. Ingham, Convective heat transfer-mathematical and computational modeling of viscous fluids and porous media. Oxford OX5 IGB, UK (2001).
- [16] C. RamReddy, P. Murthy, A. Chamkha, A. Rashad, Influence of viscous dissipation on free convection in a non-darcy porous medium saturated with nanofluid in the presence of magnetic field, *The Open Transport Phenomena Journal*, 5 (2013), 20-29.
- [17] P. Rana, R. Bhargava, O. A. *Be'g*, Numerical solution for mixed convection boundary layer flow of a nanofluid along an inclined plate embedded in a porous medium, *Comput. Math. Appl.* 64 (2012), 2816-2832.
- [18] Z. Uddin, S. Harmand, Natural convection heat transfer of nanofluids along a vertical plate embedded in porous medium, *Nanoscale Research Letters* (2013).
- [19] K. Vafai, *Handbook of porous media*, second edition. CRC press Taylor and Francis Group, New York (2005).
- [20] M. H. Yasin, R. Arifin, Mixed convection boundary layer flow on a vertical surface in a porous medium saturated by a nanofluid with suction or injection, *J. Math. Statistics*, 2 (2013), 119-128.